



STUDY OF HYDROGEOCHEMISTRY OF RIVER WATER AND ROCK SAMPLES ALONG RIVER KUSHAVATI, SOUTH GOA



A project report submitted in partial fulfilment of the requirement for the Degree of

Bachelor of Science

in

GEOLOGY

By

Afonso Samuel

Das Ashish

Goes Bevelio

Naik Sahil

Pai Prabhakar

Prabhu Shravan

Souza Alistair

Under the supervision of

Dr. Meghana Devli

Assistant Professor

**PARVATIBAI CHOWGULE COLLEGE OF ARTS AND SCIENCE,
AUTONOMOUS**

2019 -2020

DECLARATION

We declare that this project titled “Hydrogeochemistry of River Water and Rock Samples along the River Kushavati, South Goa” has been prepared by us and to the best of our knowledge; it has not previously formed the basis for the award of any diploma or degree by any other University.

Roll No.	Name	Signature
SU170174	Afonso Samuel	
SU170459	Das Ashish	
SU170372	Goes Bevelio Philip	
SU170120	Naik Sahil	
SU170083	Pai Prabhakar Sai	
SU170111	Prabhu Shravan	
SU170373	Souza Alistair	

CERTIFICATE

Certified that the Project Report titled “Hydrogeochemistry of River Water and Rock Samples along the River Kushavati, South Goa” is a work done by themselves under my guidance during the period of study and that to the best of my knowledge, it has not previously formed the basis of the award of any degree or diploma of any other University.

Date:

Dr Meghana S. Devli
Assistant Professor
Department of Geology

ACKNOWLEDGEMENT

Firstly we would like to thank Assistant Professor Dr. Meghana S. Devli for presenting the idea of this topic and guiding us in the entire proceedings of the project w.r.t. the data as well as the finances.

We thank Department of Biotechnology (DBT), Ministry of Science and Technology, Government of India for financing the project.

Special thanks to National Geophysical Research Institute (NGRI), Hyderabad for scientific services in XRF and TIC data and preparation of Rock Micro-sections.

We would like to thank the Head, Shri Harish S S. Nadkarni, Department of Geology, for allowing the use of equipment's and facilities of the department laboratory.

Due thanks are also to Laboratory Assistant, Doreen D Souza for helping with the processing of the finances.

Gracious thanks to Assistant Professor Malcolm Afonso for providing GIS assistance and Assistant Professor Magnolia Miranda for enlightening in microscopic study.

We are grateful to the Department of Physics, Parvatibai Chowgule College for providing with agate mortar for crushing of rock samples

We express our gratitude to classmate Mr. Gomes Ashwin for providing the technical support.

Finally thanks to our parents and friends who supported us during the completion of this project.

Contents

Chapter 1	1
Introduction	1
1.1 Preface.....	1
1.2 Physiography and drainage of Goa.....	2
<i>1.2.1 Physiography</i>	2
<i>1.2.2 Drainage of goa</i>	4
1.3 Geology of Goa	8
<i>1.3.1 Barcем Group:.....</i>	8
<i>1.3.2 Ponda Group:</i>	8
<i>1.3.3 Anmode Ghat trondhjemite gneiss:</i>	10
<i>1.3.4 Chandranath Granite gneiss:</i>	10
<i>1.3.5 Canacona Granite:.....</i>	10
1.4 Hydrogeochemistry.....	12
<i>1.4.1 Factors effecting water geochemistry</i>	12
<i>1.4.2 Relationship between weathering and hydrogeochemistry</i>	13
1.5 The Carbon Cycle.....	14
1.6 Literature review.....	15
<i>1.6.1 Previous studies</i>	16
1.7 Study area.....	19
1.8 Aims and Objectives.....	21

1.8.1 Aim: Hydrogeochemistry of the river water and the rock samples of River Kushavati, South Goa.....	21
1.8.2 Objectives:	21
Chapter 2.....	22
Methodology.....	22
2.1 Field data collection.....	22
2.2 Sample preparation	23
2.3 X-Ray Fluorescence (XRF).....	25
2.3.1 <i>Introduction</i>	25
2.3.2 <i>Fundamental Principles of X-Ray Fluorescence (XRF)</i>	25
2.4 Dissolved organic carbon (DOC)	26
2.4.1 <i>TOC/DOC analysis</i>	27
2.5 Total Inorganic Carbon (TIC).....	28
<i>Measurement of the TIC concentration</i>	29
Chapter 3	30
Results	30
3.1 Megascopic identification of Rocks.....	30
3.2 Study of Rock Microsections	35
3.3 XRF analysis	38
3.4 TIC and DOC data	40
Calculation for river runoff:	42
Chapter 4.....	46

Discussion.....	46
<i>4.1 Weathering of Feldspars</i>	46
<i>4.1.2 Residence time and the DIC yield</i>	50
Chapter 5	52
Conclusion.....	52
Bibliography.....	54

List of Figures

Figure 1.1: Physiography of Goa by (Source: Fernandes, 2009)

Figure 1.2: Drainage of Goa (Jayaprakash et. al. 2013)

Figure 1.3: Geology of Goa with the Sample Collection Sites (adapted from Desai, 2011)

Figure 1.4: Group members conducting Literature review

Figure 1.5: The 5 sample collection sites of the Study Area

Figure 2.1: Collection of water samples in location L3 (Sirvoi)

Figure 2.2: Sample Preparation for XRF

Figure 2.3: Observation of rock thin sections under the Binocular Petrological microscope

Figure 2.4: Packaging of samples to dispatch to NGRI

Figure 3.1: Granite Gneiss from location L1

Figure 3.2: Sandstone from L2

Figure 3.3: Sandstone from Location L3

Figure 3.4: Red Phyllite from location L3

Figure 3.5: Granite Gneiss from Location L4

Figure 3.6: Granite from Location L5

Figure 3.7: Microscopic section matrix supported Sandstone to the left and Clast supported Sandstone to the right from locations L2 and L3 respectively.

Figure 3.8: Highly altered Plagioclase of L1 observed in BXP

Figure 3.9: Deformed Plagioclase of L5 observed in BXP

Figure 3.10: In the Rocks sample of location L4;

- A. Depicts a well formed Plagioclase grain in BXP.
- B. An altered Plagioclase lath with relicts of lamellar twinning and Kaolinite observed in BXP.

Figure 3.11: Profile along the River track in Google Earth imagery indicating the average slope

Figure 3.12: The Bjerrum Plot with the Dotted line indicating the plot for Fresh water and the Solid line being the plot for Seawater (Middelburg, 2019)

List of Tables

Table 1.1: Chart of the major rivers of Goa along with the major tributaries. (Source: Watershed Atlas of India)

Table 3.1: The XRF data in percentages along with the calculated CIA and PIA percentages.

Table 3.2: The constituents of the Total Carbon

List of Graphs

Graph 3.1: Representation of maturity of rocks.

Graph 3.2: The TIC and TOC trend along the river track.

Graph 3.3: The percentages of the constituent Carbon

Chapter 1

Introduction

1.1 Preface

Over the past several years there has been a growing concern owing to the erratic change in the climate. There has been an overall rise in global temperature commonly termed as Global Warming. This being a result of the increase in Greenhouse gas emissions via Anthropogenic and natural processes. Carbon Dioxide is one of the important Greenhouse gases that contributes in Global Warming. Therefore it is necessary to study the Carbon cycle to gain a better understanding to the Carbon emission and consumption in the atmosphere.

Anthropogenic sources are known to have a severe impact in increasing the net carbon content in the atmosphere, whereas the plant and several bacterial life are known to try to maintain the CO₂ levels by consuming CO₂ for their metabolism. It is therefore necessary that the geological aspects that control the Carbon cycle be known.

This project focuses on the Hydrogeochemistry and the Geochemical weathering of the rocks along the main track of the River Kushavati by studying the total dissolved organic and inorganic carbons present in the river water as well as studying the Chemistry of the rocks along the river Kushavati. Many similar studies were conducted in various regions of the world with the underlying geology being of mafic and carbonate types. The geology being of the Pre-Cambrian silicate rocks, this research will be among the rare researches conducted in regions consisting of Granito-Gneissic rock types.

1.2 Physiography and drainage of Goa

1.2.1 Physiography

The state of Goa forms a part of the coastal tract of the mid-West coast of India.

Physiographically, Goa is segregated into three broad zones which are called the Coastal plain in the west, the Midland hilly region in the central area and the Western Ghats in the eastern border of the state of Goa.

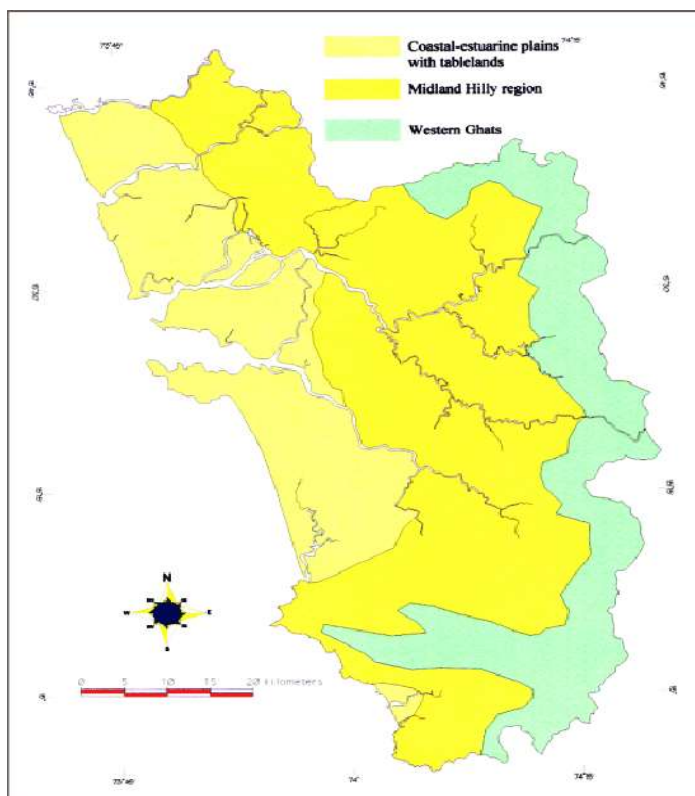


Figure 1.1: Physiography of Goa by (Source: Fernandes, 2009)

The western coastal-estuarine plain with tableland:

This terrain contains low-lying features like stretches of estuarine mudflats sandy beaches etc., widens in the north and do not stretch continuously in the southern part of Goa, being interrupted by low lying laterite topped plateau. This tableland often forms rocky headlands

leaning on the seafront and in between them lie the sandy beach stretches of the low-lying coastal plains.

The central undulating region (midlands):

This region includes relict hills ranging from approximately 100 to 600 meters and are intermediate terrain between the plateau and lower coastal plain and the steeper, higher terrain of the Western Ghats. This midland region is the border to the north because the Western Ghats are present further inland in the north Goa. The valleys and hills of this undulating region are generally aligned in a NW-SE direction. The trend of the Ghats and the hills in North Goa are operated by the structure of the rock formations in this region and are almost parallel to the coast. However in the south, the rock formations are WNW-ESE and therefore the Ghats and the hill ranges have a trend closer to East-West. As the coastline is almost North-South the East-West trending hills and the ridges come in contact with the sea at their western ends. In the Southern region of Goa, it is tough to demarcate the midlands from Western Ghats because of the transition from the rugged coastline to mountain ridge tops is very sharp.

The Western Ghats:

This hilly region consists of higher (600 to 1000 meter high) and steeper ranges and covers the eastern and the southern part of Goa. The Western Ghats have a general NW-SE trend (except in the ranges in south Goa). In north Goa it is more than 40 km away from the sea. In south however, the trend of the hills, which is related to the lower lying rock structure, is almost East-West (WNW-ESE). Here, a Western part of the Ghats (Karmal Ghat) which literally meets the sea in its lower reaches. As a result, the talukas of Canacona and Quepem

have very less areas of the coastal estuarine plain and the midland region translates very sharply into the Ghat region.

1.2.2 Drainage of goa

All the rivers that drain the state of goa flow westwards. The most important of these rivers are the Zuari and the Mandovi, that cover 26.28% and 42.68% of the total drainage of Goa. The High hill ranges of the Western ghats in the East of Goa form the main watershed. The streams originating here flow in the Westerly and North-Westerly direction to reach the Arabian Sea. The river Tiracol forms the Northern Boundary of the Goa state and separates Goa from Maharashtra. The other small rivers draining Goa are Chapora, Tiracol, Sal, Galgibaga, Talpona, Baga, Saleri.

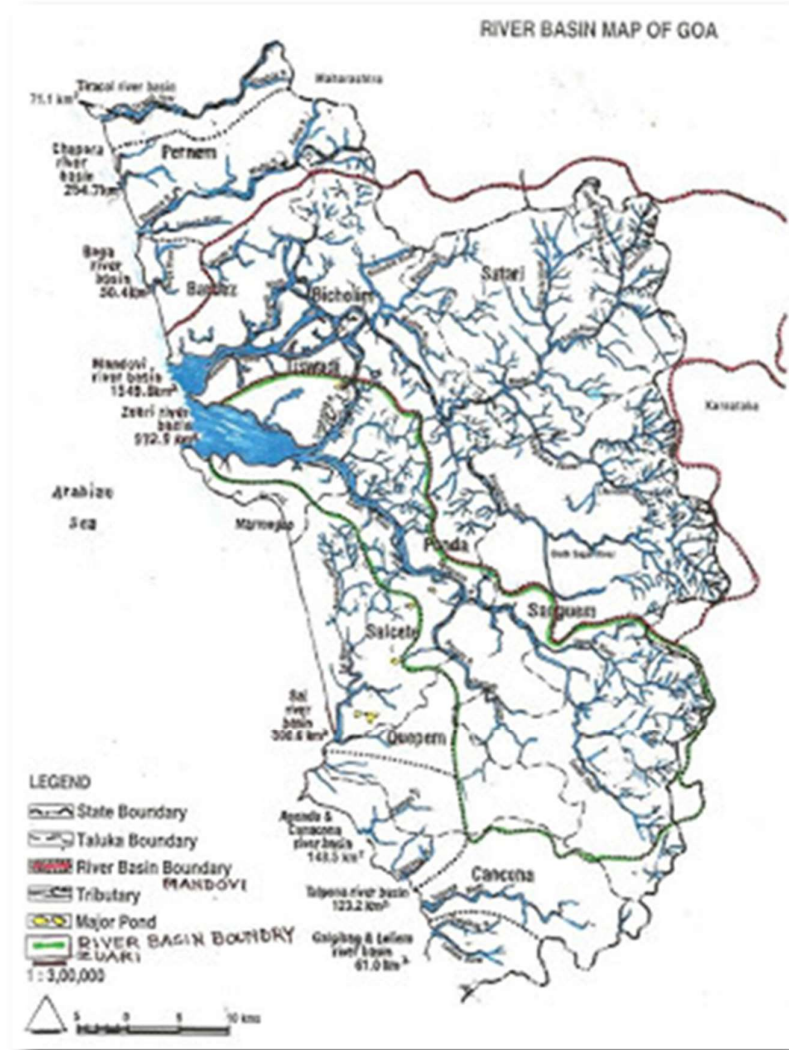


Figure 1.2: Drainage of Goa (Jayaprakash et. al. 2013)

Most of the streams originating in the Western Ghats either join some of the major rivers or directly flow westwards and drain into the sea. The Uguem and Guloli rivers flows from the highlands and joins to form the Sanguem River, which flows in a northwesterly direction to form the Zuari River. The Kushavati and the Kumarzuva are the other tributaries of the zuari, the latter meeting the Zuari at Sankawali. The Sal river flows parallel to the coast to meet the Arabian Sea near Betul. Major portion of the state is drained by the two rivers, viz. River

Mandovi and river Zuari. The other smaller rivers draining the state are Talpona, Chapora, Galgibag, Saleri, Sal and Baga.

The river Tiracol forms the northern boundary of Goa and separates it from Maharashtra. It is known as the Banda river in the upper course and Tiracol in its lower course. It originates in Manohargad in the Western Ghats and follows a south-westerly trend and finally opens up in the Arabian sea. Similar to river Tiracol, the Chapora river originates near Ramghat in the Western Ghats region of Maharashtra and flows westwards to the Arabian sea.

The Mandovi originates from a cluster of 30 springs in Bhimgad in the Western Ghats, in the Belagavi district of Karnataka. It is the largest river of Goa having 42.68% of the state's catchment area. The Zuari is the second largest river of Goa having 26.28% of the catchment area of Goa. The Sal river is a small river originating from several springs in Nuvem, it then flows towards the South and opens to the Arabian sea in Betul. The Talpona River originates in the dense, mixed pristine jungles of Ravan Dongar in between Nane and Kuske on the Sahyadri Mountains of Goa. (NGT appointed panel proposes Talpona River rejuvenation, 2019)

Sl.No.	Basin Name	Place of origin of main river	Catchment area		Major Tributaries
			Total	In Goa	
1	Terekhol	In western Ghats in Sawantwadi Taluk of Maharashtra	71	-	
2	Chapora	Sawantwadi Taluk of Maharashtra	255		Kalna & Arabo
3	Baga	Bardez Taluk, Goa	50	50	-
4	Mandovi	Khanapur Taluk, Karnataka state	1580		Madei & Khandepar
5	Zuari	Western Ghats on eastern boundary	973	973	Salauli, Ugem & Kushvati
6	Sal	Salcete taluk, Goa	301	301	
7	Saleri	Quepem taluk, Goa	149	149	
8	Talpona	Western Ghats on eastern boundary	233	233	Goandongarem & Kuske
9	Galgibag	Western Ghats on eastern boundary	90	90	-
Total			1796	3702	

Source: Watershed Atlas of India, all areas are in Sq.km.

Table 1.1: Chart of the major rivers of Goa along with the major tributaries. (Source: Watershed Atlas of India)

The drainage system of Goa is governed by the underlying rocks. The drainage pattern is usually dendritic depending upon the underlying geological formations, but the trend of the rivers is guided by the structural lineament. The river Zuari follows the major North-West synclinal axis. The river valleys are generally V-shaped as the rivers cut through the Western Ghats and broaden in the midlands and are U-shaped near the plains and the lowlands where the strength of the river is reduced. The drainage density decreases when the rivers flow from highlands (East) to midlands and then to the estuaries (West) where they open to the Arabian Sea. The cross profiles of most of the rivers of Goa including the Zuari and Sal is nearly flat in most of their lengths. Conversely, the cross profile of some like the Kushavati, the Guloli, the Uguem, etc, are typically V-shaped. (Jayaprakash, Sooryanarayana, Davithuraj, & Sivaramakrishnan, 2013)

1.3 Geology of Goa

“The Geology of Goa Group: Revisited” infers that the supracrustals containing the Goa Group of Gokul et al, can be separated into two lithostratigraphic sequences namely the Ponda Group and the Barcem Group. The older group i.e. the Barcem Group, rests on a Basement of 3300-3400 Ma Anmode Ghat trondhjemite gneiss.

1.3.1 Barcem Group:

The newly classified Barcem Group is best developed to the southeast of the Barcem village and account for a thickness of over 2 km. It has a quartz-pebble conglomerate below it and the lithounits compose of metavolcanics with intercalations of quartzites and pilites. The volcanics are exhibited by basic and felsic lavas, agglomerates and tuffs. The metasediments compose of quartzites, quartz-sericite-schists, quartz-chlorite-schists and minor phyllites. Non-vesicular metabasalts as well as vesicular metabasalts are exposed in certain regions.

1.3.2 Ponda Group:

The Ponda Group is best developed around the town of Ponda where most of the lithologies are seen. This group consists of three formations namely: the Sanvordem Formation, Bicholim Formation and the Vagheri Formation which are in ascending order.

Sanvordem Formation: This formation is the oldest of the three formations. The Sanvordem Formation lies over the Chandranath granite gneiss with a polymict metaconglomerate underlying it and consists of metagreywacke and agrellites. The conglomerate contains stretched and elongated pebbles of quartzite and gneiss in a schistose chlorite matrix. The

most significant section of this formation is exposed along the railway tract between Sanvordem railway station. In this section it has a thickness of over 1.2 km.

Bicholim Formation: This Formation can be found over the entire length of Goa (~ 185 km) in a NW-SE direction from Naibag in the northwest to Salgini in the southeast. The average true thickness of the Formation is around 1.4 km. It comprises of ferruginous, amphibole schists and manganiferous phyllites, limestones and banded ferruginous quartzites (BHQ) that occur as intercalations within the phyllites. The BHQs serve as the proto-ores for the iron ore deposits that are extensively developed in this formation. Calcareous (carbonate facies of BIF) and carbonaceous (sulphide facies) intercalations are common. Manganese being an inseparable associate of iron in almost all BIF, both these show a zonal distribution pattern.

Vagheri Formation: The youngest formation of this particular Group is shown by the Vagheri Formation which conformably overlies the Bicholim Formation. It is best exposed to the northeast of Valpoi. It comprises of metagreywacke-argillite with intercalated metabasalts. The metagreywackes are grey to greyish green, compact and show poorly developed schistosity. The rock comprises of angular to sub-angular crystic- and lithic-fragments in a fine grained mesostasis made up of quartz, chlorite and feldspar. The rocks are immature with poorly sorted angular and subangular clasts of andesitic tuffs. The metabasalts occur as narrow, lenticular intercalations within the metagreywacke and show a poorly developed foliation at some places. The supracrustal sequence is intruded by the Bondla layer of mafic-ultramafic complexes along a major shear zone (NW-SE) that controls the course of tributary of River Mandovi flowing in N-W direction. The late Canacona granite intrusion marks the close of sedimentation in the Goa basin.

1.3.3 Anmode Ghat trondhjemite gneiss:

The gneiss is exposed at Anmode along the Panjim-Belgaum national highway and is amongst the oldest gneisses from India. Anmode Ghat trondhjemite gneiss is fine grained, granulated and has a metamorphic fabric. This is the oldest rock present in Goa.

1.3.4 Chandranath Granite gneiss:

It is a grey granitic gneiss that shows variation in composition from granodiorite to quartz-diorite. Recent SmNd isotope studies provide model ages of about 2900 Ma showing that the protoliths are either younger than the trondhjemites or are less enriched in light rare earth elements. They form the basement for the Sanvordem Formation of the Ponda Group. The relationship between the gneiss and the supracrustal assemblage is best exposed to the east of Sanvordem railway station where the metaconglomerate with granite-clast unconformably overlies on the gneiss and contains stretched pebbles of granitic gneiss along with those of vein-quartz in a chlorite-rich matrix.

1.3.5 Canacona Granite:

It is exposed at Char Rasta-Chauri, Palolem and Agonda, in Canacona taluka. With reference to the latest geological and mineral map of Goa, the granite is depicted as intrusive into the TTG gneisses. It has been dated at 2395 ± 390 Ma, however, because of large error factor, the age information is a suspect. The granite is distinctly late, unfoliated, and shows a discordant relationship with the WNW-ESE foliation of the older TTG gneiss/migmatite.



Figure 1.3: Geology of Goa with the Sample Collection Sites (adapted from Desai, 2011)

1.4 Hydrogeochemistry

Hydrogeochemistry is defined as the chemistry of ground and surface waters. Significantly their relationship between the chemical characteristics and quality of waters and areal and regional geology.

The two main processes responsible for effecting the hydrogeochemistry of water, mainly groundwater are weathering and anthropogenic activities. Continental waters are the most common agents that weather rocks and transform landscapes. Water chemistry is the by-product of interactions amongst infiltrating water (rain or surface water) and rocks. Water plays a significant role:

1. As a chemical reagent, dissolving minerals and organic matter, and
2. As a transport agent of energy and mass.

Hydrogeochemical studies are significant in groundwater sciences, mostly because they allow the palaeohydrogeology to be investigated. Hydrogeochemistry is hence of significant use in reconstructing past groundwater circulation under ice sheets as the meltwater recharging the subsurface has a geochemical signature that can be differentiated from other sources of water generated under warmer climates.

1.4.1 Factors effecting water geochemistry

The chemical content of water depends on three major factors,

1. The rock type i.e. the mineralogy and the grain size in contact with the flowing water.
2. The environmental conditions that include the climatic conditions, which in turn determine the flow rate, the temperature and the pressure.

3. The flow conditions that determine the gaseous phase and the time is an important factor for water-rock dissolution. The longer the water-rock contact, the more mineralized the water.

The water chemistry in its simplest form involves two and three aspects which include; the water-rock and the gas-water-rock systems. The three-phase systems are more complicated, as it involves more reactions and equilibrium.

1.4.2 Relationship between weathering and hydrogeochemistry

Mechanical weathering physically breaks down rocks because of environmental factors that include heat, cold, water and wind. This type of weathering has no effect on the hydrogeochemistry. One effect of chemical weathering is hydrolysis. Through hydrolysis, water gets added into the chemical structure of a mineral, which turns the mineral into a new one. For example, hydrolysis changes feldspar into clay. Because water is a catalyst in chemical reactions, chemical weathering occurs mostly in areas with plenty of water and high temperatures. Carbonic acid is a major contributor to the weathering of the exposed rocks. The source of this acid is the atmospheric carbon which combines with water to form weak acid. The acid then dissolves the minerals present in the rocks; also known as chemical weathering resulting in the release of Ca^+ , Mg^{2+} , K^+ or Na^+ ions which are carried by rivers into the sea. It tends to be common in hot and humid tropics.

1.5 The Carbon Cycle

The dissolved inorganic carbon which is part of the Total inorganic carbon, is available in water in three forms: CO_2 , HCO_3^- , CO_3^{2-} . The pH values of the water depends on the concentration of these species. The pH would be 9 if all the CO_2 was used up. The pH would be 11 if all HCO_3^- would have been used up by the plants having the enzyme Carbonhylase.

The most important input for the DIC is the solution of atmospheric CO_2 , underground pool, inorganic carbon bound in sediments, the biological and chemical processes. The dissolved organic carbon pool contains a mixture of substances. Besides other allochthonous inputs, secretion and excretion and autolysis of the detritus are the most important sources for DOC. The uptake by bacteria is the most essential output. POC is changed by respiration into DIC and by excretion, secretion and autolysis into DOC.

Aquatic plants consume DIC by:

1. Forming leaves.
2. The using the CO_2 in the water of the sediment.
3. Forming of C^4- metabolism enabling them to fix CO_2 during night time.

The most important pools for carbon in an aquatic environment like a lake or a river include the following:

1. Dissolved organic carbon.
2. Dissolved inorganic carbon.
3. Particulate organic carbon.

1.6 Literature review



Figure 1.4: Group members conducting Literature review

One of the major concern among the current generation is the issue of climate change. The rise in the average temperature of the earth have led to initial signs of catastrophe; the major one being the melting of glaciers and ice caps which in turn results in the rise in sea levels. The major cause of this Global Warming is the increase in Greenhouse gases with the prominent one being CO₂. This has laid the emphasis on the study of the Carbon Cycle which is basically the interaction of carbon between the various Spheres of the Earth (Geosphere, Hydrosphere, Atmosphere and Biosphere). The organic carbon cycle within the biosphere which is one component of the larger carbon cycle is known to have effects on the climate (Berner & Lasaga, 1989). Human interaction is known to have created an imbalance in the carbon cycle leading to increase in the net atmospheric carbon content. The burning of fossil fuels has increased the CO₂ content and the depletion of trees has led to lower consumption rates of the atmospheric carbon.

The cycle that includes the geochemical weathering aspect is known to affect the atmospheric CO₂ content over geological time scales (>1My). Its effects on shorter timescales is arguable (Frondini, Vaselli, & Zuccolini, 2019). To enhance our knowledge on the relation between the chemical weathering of rocks and the atmospheric CO₂ various studies have been conducted along water shed areas as these rocks are most susceptible to geochemical weathering. The carbon is principally stored in sedimentary rocks as carbonates in limestones and dolomites and as Kerogen which is basically the organic carbon. The chemical weathering depends on various factors like temperatures, lithology, runoffs and the pH of the water. The carbonic acid weathers carbonate rocks as well as silicate rocks and result in production of bicarbonate ions. This is then transported into basins (oceans) through groundwater and rivers to give rise to rocks like Calcium carbonate by the interaction of planktons, corals and other marine organisms. The source of this carbonic acid is the atmospheric carbon. In the chemical weathering of silicate minerals like feldspars in granites and basalts; the source of the bicarbonate ions is only the carbonic acid indicating the importance of silicate weathering to control the atmospheric carbon content (Berner & Lasaga, 1989). These weathering processes behave as carbon sinks. The preceding researches in localised areas have been conducted to study the carbon dynamics and the effects of geochemical weathering on the atmospheric carbon. Two examples are included considering both the rock types; the chemical weathering carbonate rocks and the Basalts (silicate minerals).

1.6.1 Previous studies

The outcrop cover of carbonate rocks ranges from 9-16% of the continental area and are major sources of the Dissolved Inorganic Carbon (DIC) (CAO, et al., 2012). According to a study in the Yangtze River Basin in China which is predominant of carbonate rocks and the

third largest river in the world, the average consumption rate of atmospheric CO₂ is 20.6 t/km² per year. Unlike the common catalysis for geochemical weathering being the carbonic acid, the weathering in this basin is also due to sulphuric acid which has increased the rate of carbonate rock weathering by 28% decreased the consumption rate of CO₂ by 12%. The sulfuric acid causing this increased rate of weathering is from anthropogenic sources (Zhang, Qin, Huang, & Liu, 2019).

The principal process by which CO₂ is consumed from the atmosphere is by the Chemical weathering of Ca-Mg silicate rocks (Berner, Weathering, plants, and the long-term carbon cycle, 1992). The watershed systems present in the Voltri Massif in Italy because geochemical weathering of the ultramafic rocks present in the area. The results indicate the CO₂ consumption to be 96.13 t/km² per year which is higher than the Average CO₂ consumption of the world. In this study it was concluded that the chemical weathering of the ultramafic rocks form one of the most influential carbon sinks. The snow melting due to the increased temperatures will lead to higher runoffs ultimately leading to higher consumption of CO₂ (Frondini, Vaselli, & Zuccolini, 2019).

Studies of chemical weathering of the silicate mineral bearing rocks were also conducted in the 70 tropical rivers in the Western Ghats of India. The rocks in the Western Ghats include the Deccan traps (DT) which are basaltic, the Western Dharwar Cratons (WDC) and the Southern Granulite Terrain (SGT) which are metamorphic and granite dominated. The tropical rivers in this region cause intense chemical weathering of the silicates and globally has the 9th largest DIC yield. The rate of DIC yield approximates to 492.42 t/km² per year (Reddy, Gupta, & Reddy, 2019).

Increased atmospheric CO₂ creates higher temperatures, greater precipitation and higher runoff which is ideal for increased silicate rock weathering. This increase in silicate weathering will result on depleting atmospheric CO₂ over time therefore stabilizing atmospheric CO₂ (Berner & Caldeira, The need for mass balance and feedback in the geochemical carbon cycle, 1997). But according to a study, Global Warming and Acidification is not restricted to rivers but to the oceans. The oceanic acidification is due to the increased supply of DIC. This leads to decalcification and emission of CO₂ from the carbonates, corals, foraminifera and benthic life (Kawahata, et al., 2019).

To enhance the knowledge of the effects of chemical weathering of the silicate rocks, the geochemical study will be conduct along the course if the river Khushavati which is located near the Western Ghats and consist the silicate rocks of the Western Dharwar Craton.

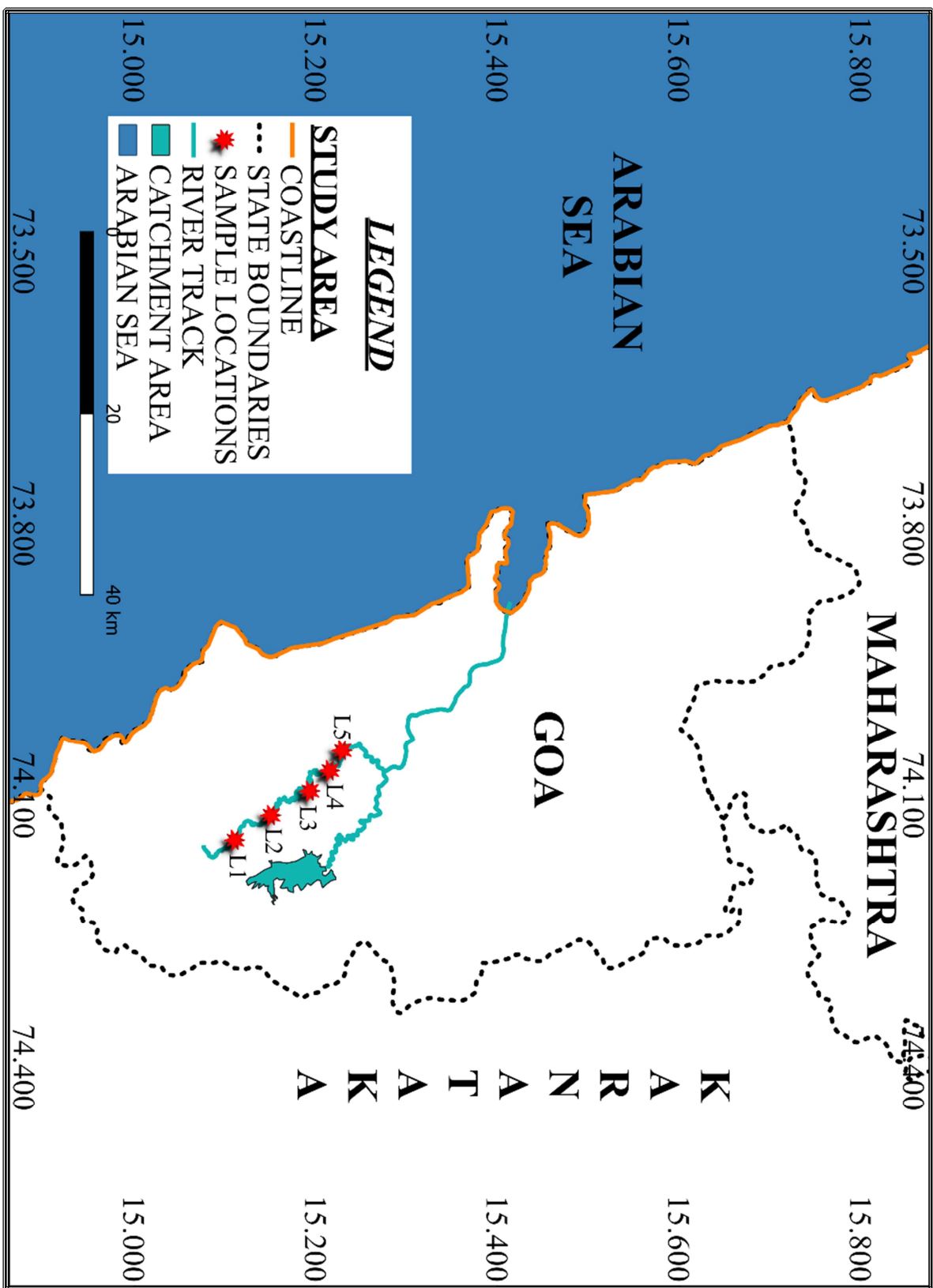
1.7 Study area

The state of Goa consist of nine major rivers with each river having its tributaries. These tributaries contribute to the drainage of these major rivers. For the purpose of studying the hydrogeochemistry of the Precambrian silicate rocks of the Dharwar Craton and its effects on the atmospheric carbon, the River Khushavati was chosen, which is in the South Goa District, in the Talukas of Salcette and Quepem. The River Khushavati is the major tributary of the second largest river in Goa i.e. the River Zuari. The average width of the River Kushavati amounts to 33 metres with the length of the river course being 43 kilometres. The watershed of the river amounts to 661 km². This was calculated using Google Earth imagery. The study area was conducted in five different spots - tagged as L1, L2, L3, L4 and L5 - along the main track of the River Kushavati, each at an approximate distance of 4-8 km with the distance between L1 and L5 being 30 km approx. The villages of the Sample collection sites are; Sulcorna, Rivona, Sirvoi, Quepem Town and Chandor in ascending order towards downstream. These locations were chosen based on the criteria of:

1. Proximity to the Parvatibai Chowgule College
2. Easy accessibility to the Outcrop
3. The comparably shallower depth of the river helping in safer collection of water samples

From each location three samples had to be collected which included the:

1. Unfiltered Water samples for total carbon analysis
2. Filtered Water samples for dissolved carbon analysis and
3. Rock samples for XRF analysis, Petrography and calculation weathering trends



1.8 Aims and Objectives

1.8.1 Aim: Hydrogeochemistry of the river water and the rock samples of River Kushavati, South Goa.

1.8.2 Objectives:

- Collection of the rock and water samples by field studies
- Preparation of rock micro-sections for petrography
- Detection of major oxide composition using X-Ray Fluorescence (XRF)
- To interpret the weathering trend of the rocks along the River Kushavati
- To study the carbon flux by conducting organic carbon and inorganic carbon analysis

Chapter 2

Methodology

2.1 Field data collection



Figure 2.1: Collection of water samples in location L3 (Sirvoi)

Three types of samples were collected; Unfiltered Water samples, Filtered Water samples and rock specimen. Each collected from five different locations - named as L1, L2, L3, L4 and L5 - along the main track of the River Kushavati, each at an approximate distance of 4-8 km with the distance between L1 and L5 being 30 km approx. The filtered water samples were collected for the procurement DIC, DOC data and the unfiltered water samples were collected for TIC, TOC and TC analysis, to study the carbon flux. The rock samples were collected for thin sections and for X-Ray Fluorescence. The thin sections were used to analyse the rock type and for the identification of the mineral composition. X-Ray fluorescence is used to identify the oxide components present in the rock to calculate the alteration trend, rock chemical maturity and the plagioclase content. Megascopic identification of the rocks were also conducted for the petrological study.

2.2 Sample preparation



Figure 2.2: Sample Preparation for XRF

The two types of water samples were collected in PVC bottles; one being filtered and the other being unfiltered. The rock samples were collected by manual methods of geological field work. The purpose for collection of these rock samples were for three modes of analysis. One was for the study and identification of the rock types and the minerals by megascopic practices. Thin sections of the specimen for mineral identification and studying the alteration products; for which the rock samples were demarcated along certain planes for observing those microscopic sections along those planes for petrographic analysis. These samples were named as L1, L2, L3, L4 and L5 according to the location of the sample collection sites.



Figure 2.3: Observation of rock thin sections under the Binocular Petrological microscope

These tagged specimen were also crushed to finesse i.e. to the finest possible grain size by manual methods using an agate mortar; which were for XRF studies. All these prepared samples were sent to National Geophysical Research Institute (NGRI) to conduct the required analysis and to procure the data.



Figure 2.4: Packaging of samples to dispatch to NGRI

2.3 X-Ray Fluorescence (XRF)

2.3.1 Introduction

The chemical analyses of minerals, rocks, sediments and fluids for elemental analysis using an X-Ray instrument by regular, non-destructible methods is known as an X-ray fluorescence (XRF) spectrometer. It works on the principle of wavelength-dispersive spectroscopy which basically the scattering of the x-rays on interaction with the elements. The typical use of XRF is for the bulk analyses of larger samples of geological materials as it is not compatible for spot analysis. This is one of the most widely used methods for analysis of major and trace elements in rocks, minerals, and sediment.

2.3.2 Fundamental Principles of X-Ray Fluorescence (XRF)

The analysis of major and trace elements in geological materials by x-ray fluorescence is possible due to the response of atoms after their interaction with radiation. The analysis of major and trace elements in geological materials by XRF is possible due to the behaviour of atoms after their interaction with X-radiation.

After the excitement of atoms due to high energy, short wavelength radiation of the X-rays, there is a probability of them being ionized. If the energy of the radiation is enough to release a strongly-held inner electron, the atom gets unstable and an outer electron takes the place of lacking inner electron.

Due to this there is a decrease in binding energy of the inner electron orbital compared with an outer one which leads to the release of the energy. The emitted radiation is of lower energy

compared to the primary incident X-rays and is described as fluorescent radiation. Because the energy of the released photon is feature of a modulation among particular electron orbitals in a specific element, the fluorescent X-rays resulting from this, is useful in detecting the abundances of elements found in the sample.

X-ray fluorescence is contained to analysis of;

- Comparatively large samples, generally > 1 gram
- Materials that can be made in powder form and homogenized
- Materials for which compositionally alike, well-characterized standards are present
- Materials having high abundances of elements of which absorption and fluorescence effects are well understood.

2.4 Dissolved organic carbon (DOC)

Total Organic Carbon is the carbon that is derived from organic sources that include plants as well as animals. Dissolved organic carbon (DOC) is the part of total organic carbon that can pass through a filter size of 0.45 micrometres (μm). The fraction remaining on the filter i.e. the organic carbon larger than $0.45 \mu\text{m}$ is called Particulate Organic Carbon (POC). DOC is abundant in the marine and freshwater environment and are one of the highest cycled reservoirs of organic matter on Earth. This carbon accounts for the same amount of carbon as that of the atmosphere and up to 20% of all the organic carbon. Generally, organic carbon compounds results from the decomposition processes of dead organic matter like plants and animals. DOC can be sourced from within or external to the water body. DOC that originates within the water body is known as autochthonous DOC with its source mostly from aquatic plants or algae. The DOC originating from external sources i.e. from outside the body of

water is known as allochthonous DOC and typically originates from soils or terrestrial plants. When water comes from land areas that consist of a high proportion of organic soils, the Organic Carbon can drain into rivers and lakes as DOC. Substances bound in organism and the detritus is present in the form of particulate organic carbon (POC). The main source for POC is the primary production.

2.4.1 TOC/DOC analysis

Total and Dissolved organic carbon can be measured by several different techniques. One such method id the UV/persulfate oxidation method. For this the sample has to be prepared using the following procedure:

1. The sample is collected in pre-baked glass containers which are free of previous residual carbon present on the vessel thus avoiding contamination.
2. The filtered samples are used for DOC analysis and unfiltered samples are used for TOC analysis.
3. After collecting the samples, it should be stored in a cool place until they can be processed. The processing should be as soon as possible to prevent post-filtering sample alteration.
- 4.

Method for measuring TOC/DOC by UV/Persulfate Oxidation:

The pH of the sample is reduced to 2.0 by addition of acid so as to remove the inorganic carbon by converting the inorganic carbon to dissolved CO₂, which is then purged from the sample. A persulfate reagent is then added to the sample and the remaining carbon is oxidized by UV radiation to form CO₂, which is then detected by the Non-Dispersive Infrared (NDIR)

sensor and directly correlated to as total organic carbon (TOC) or dissolved organic carbon (DOC) content.

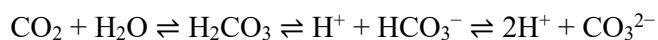
2.5 Total Inorganic Carbon (TIC)

Analogous to the TOC and the DOC the total inorganic carbon (CT or TIC) includes the dissolved inorganic carbon (DIC) as well as the particulate inorganic carbon (PIC). The source of this carbon is from minerals present in rocks and the atmosphere. This carbon is the sum of inorganic carbon species in a solution that include carbon dioxide, carbonic acid, bicarbonate anion, and carbonate.

$$CT = [CO_2^*] + [HCO_3^-] + [CO_3^{2-}]$$

- Where; CT is the total inorganic carbon
- $[CO_2^*]$ is the sum of carbon dioxide and carbonic acid concentrations ($[CO_2^*] = [CO_2] + [H_2CO_3]$)
- $[HCO_3^-]$ is the bicarbonate concentration and
- $[CO_3^{2-}]$ is the carbonate concentration

To maintain chemical equilibrium these species are related to each other by the following equation:



DIC is very important for measurements of pH parameters of natural aqueous environment, and the carbon dioxide flux estimates. The pH was calculated using pH paper strips. The concentrations of the DIC species is calculated using the pH of the water, with respect to the Bjerrum plot which is basically a graphical representation of the concentrations of the DIC species vs the pH at equilibrium state.

Measurement of the TIC concentration

The acidification of the sample converts the TIC to CO₂. This gas is then sparged from solution and trapped for measurement by infrared spectroscopy i.e. by NDIR.

Chapter 3

Results

3.1 Megascopic identification of Rocks

The rocks samples collected for the study are were studied for the megascopic as well as microscopic studies. They were identified based on their structures and textures present in the specimens.

The rock samples collected from the five locations were analysed and concluded the following:

1. At location L1 (Sulcorna):



Figure 3.1: Granite Gneiss from location L1

Based on megascopic identification the minerals identified were:

Mineral identified	Diagnostic properties
Feldspar	White Colour, Vitreous to Pearly Lustre, 1-2 sets of Cleavages
Quartz	Colourless to White, Vitreous Lustre, devoid of cleavages, Conchoidal Fracture
Biotite	Brown colour, Flaky habit, Pearly lustre
Pyroxenes/Amphiboles	Dark coloured, Prismatic/Elongated, Vitreous Lustre.

The differentiation of the felsic and mafic minerals is due to the high grade of metamorphism; and thus exhibits a Gneissic texture. Based on this mineral content and the Gneissose structure observed of light and dark minerals, the specimen is a Granite Gneiss.

2. At location L2 (Rivona):



Figure 3.2: Sandstone from L2

The minerals identified are:

Mineral Identified	Diagnostic Properties
Quartz	Colourless to White, Vitreous Lustre, devoid of cleavages, Conchoidal Fracture
Feldspar	White Colour, Vitreous to Pearly Lustre, 1-2 sets of Cleavages

The minerals grains are clastic in nature and are Sand sized. Hence the rock specimen is Sandstone.

3. At location L3 (Sirvoi)



Figure 3.3: Sandstone from Location L3

Two rock samples were collected from this location. Having properties similar to that of L1, one rock sample was identified as a Sandstone. The mineral content was dominantly Quartz.



Figure 3.4: Red Phyllite from location L3

The distinct property of the other rock sample is the presence of foliations. The rock mostly consists of micaceous minerals like Muscovite; identified by the flaky habit and pearly lustre. Some opaque minerals are also present indicated by the red colour confirming the presence of iron. The specimen is a Red/Ferruginous Phyllite.

4. At location L4 (Quepem Bridge)



Figure 3.5: Granite Gneiss from Location L4

The acquired sample was similar in appearance to the one collected from L1. It consisted of felsic minerals like; Feldspars and Quartz and mafic minerals like Biotite and Pyroxene. The rock is deformed, having a Gneissose structure with bands of light and dark coloured minerals. The texture is foliated i.e. gneissic as the felsic and mafic minerals are segregated. Therefore the specimen is a Granite Gneiss.

5. At location L5 (Paroda)



Figure 3.6: Granite from Location L5

The rocks sample from Paroda consisted of dark coloured minerals like Pyroxenes Amphiboles and Biotite and also some amount of Plagioclase. Therefore the procured specimen is identified as Dolerite.

3.2 Study of Rock Microsections

For studying and the identification of Plagioclase, rock micro-sections were prepared.

This was required to confirm the effect the weathering of these rocks had on the carbon consumption. As weathering of plagioclase can contribute Ca^{2+} cation which in turn can react with CO_3^{2-} anion in the deep oceans to give rise to carbonate rocks like (limestone), thus behaving as a carbon sink.

Plagioclase were identified based on the distinguishing microscopic properties which include:

1. In Plane Polarised Light (PPL): Colourless, Elongated/Lath shape, 1-2 sets of cleavages and Low Relief.
2. In Between Crossed Polars (BXP): Anisotropic, Grey of 1st order interference colour, Oblique Extinction and Polysynthetic/Lamellar twinning.

Plagioclase was identified in almost all the samples except in the specimen of L2 and L3 which composed dominantly of Quartz which showed undulose extinction.

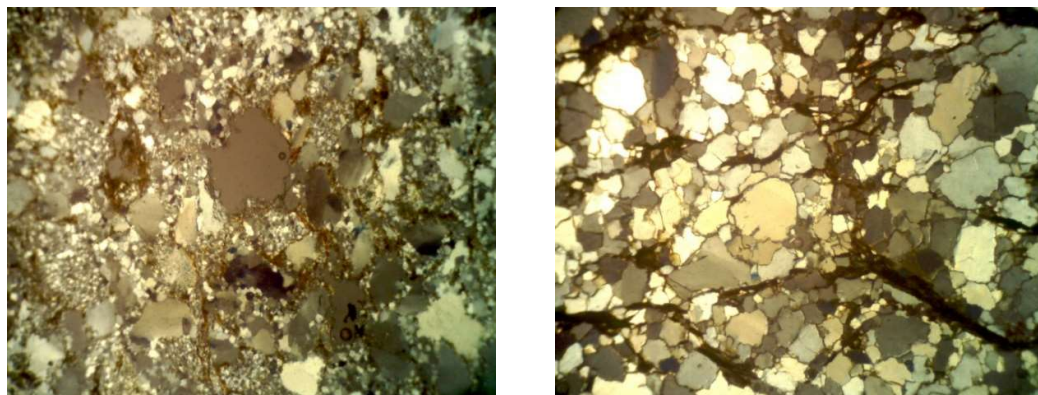


Figure 3.7: Microscopic section matrix supported Sandstone to the left and Clast supported Sandstone to the right from locations L2 and L3 respectively.

The thin sections of the locations L1, L4 and L5 had considerable amount of plagioclase. The L1 section observed under the microscope was highly altered with relicts of the plagioclase visible.

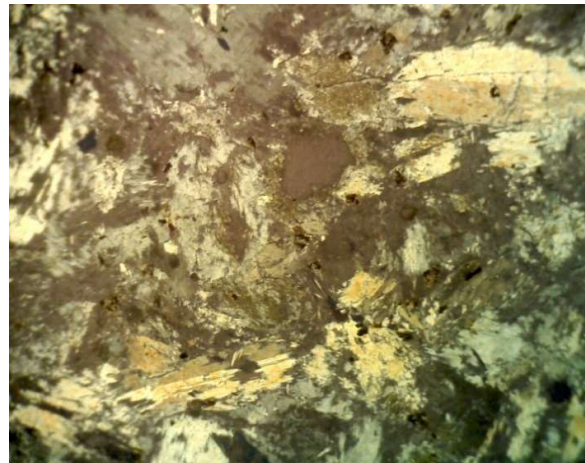
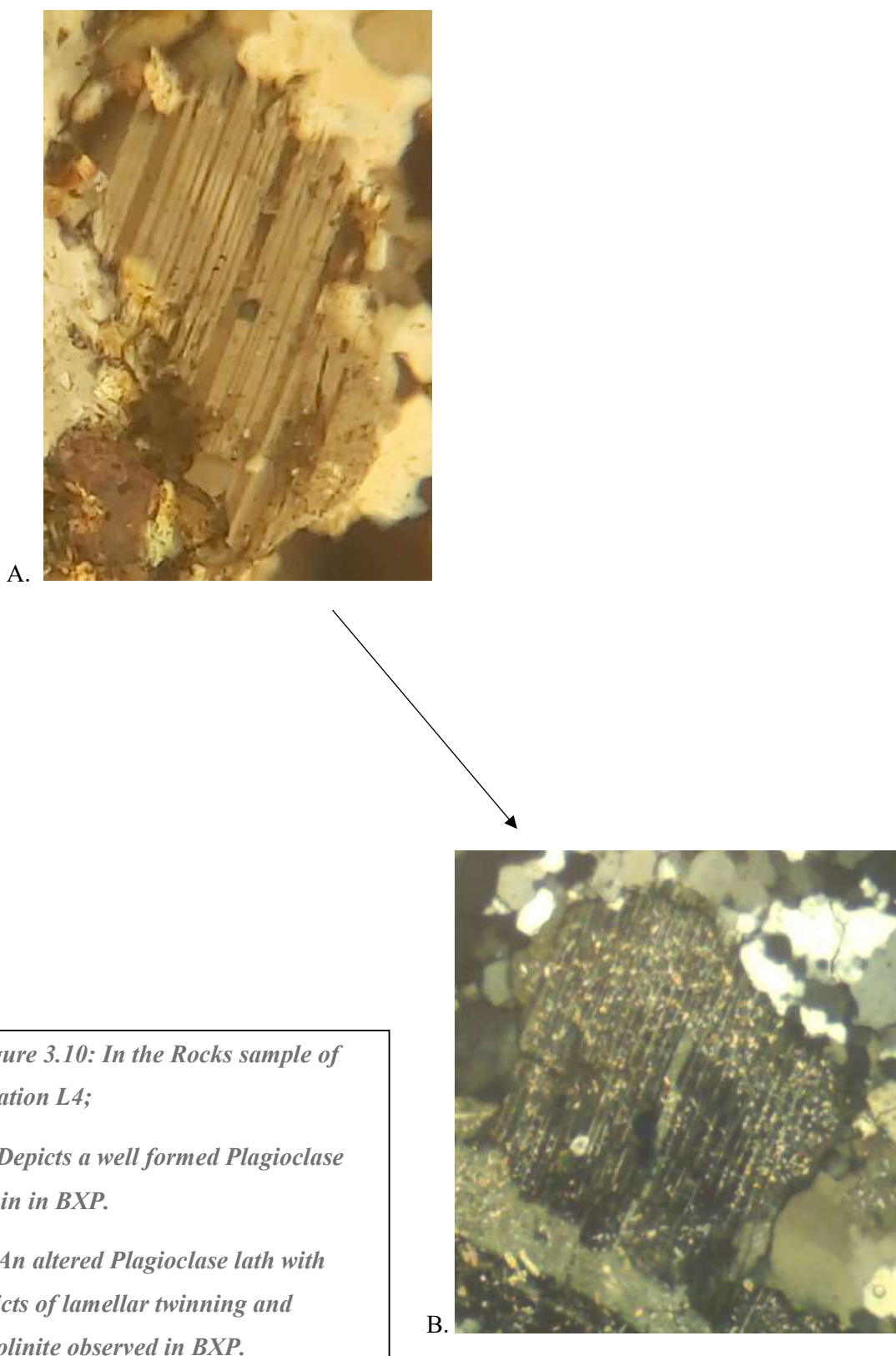


Figure 3.8: Highly altered Plagioclase of L1 observed in BXP



Figure 3.9: Deformed Plagioclase of L5 observed in BXP

The plagioclase in location L5 depicted deformation microstructures with the lamellae pinching out and having a degree of folding/bending, thus indicating stress.



3.3 XRF analysis

The data of the XRF included the major oxide compositions. This data were in percentages which were used to calculate the molecular proportions. This in turn was to calculate the weathering indices; Chemical Index of Alteration (CIA) and Plagioclase Index of Alteration (PIA) of the rock samples acquired from the locations.

Table 3.1: The XRF data in percentages along with the calculated CIA and PIA percentages.

Sample	SiO ₂	Al ₂ O ₃	Fe ₂ O ₃	MnO	MgO	CaO	Na ₂ O	K ₂ O	TiO ₂	P ₂ O ₅	CIA (%)	PIA (%)
Location	(%)	(%)	(%)	(%)	(%)	(%)	(%)	(%)	(%)	(%)		
L-1	73.70	14.27	1.34	0.02	0.39	1.59	4.47	3.21	0.20	0.05	51.196478	51.5941
L-2	90.90	3.54	2.66	0.01	0.35	0.08	0.06	0.44	0.15	0.01	84.205539	94.1393
L-3	83.52	8.82	4.38	0.03	0.56	0.10	0.52	0.05	0.15	0.03	89.666428	90.1342
L-4	72.60	15.87	0.00	0.00	0.06	0.41	3.92	5.50	0.04	0.01	54.732716	58.03
L-5	66.26	16.33	5.23	0.03	1.56	1.20	7.98	0.17	0.52	0.25	52.299772	52.327

The Molecular proportions of the constituent oxides is given by

$$= \frac{\text{Percentage of the Oxide} (\%) * 1000}{\text{Molecular Weight of the oxide} (\frac{g}{mol})} \quad (\text{Normative Calculations})$$

For Example; the molecular proportion of SiO₂

$$= \frac{73.70 * 1000}{60}$$

$$= 1228.283333$$

Using the Molecular proportions;

$$\text{CIA} = \frac{\text{Al}_2\text{O}_3 * 100}{\text{Al}_2\text{O}_3 + \text{Na}_2\text{O} + \text{K}_2\text{O} + \text{CaO}} \quad (\text{Nesbitt \& Young, 1982})$$

For Example, in the case of Rock Sample from L1

$$\text{CIA} = \frac{139.94 * 100}{139.94 + 72.09 + 34.09 + 27.22}$$

$$= 51.19 \%$$

Similarly, PIA = $\frac{(Al_2O_3 - K_2O) * 100}{(Al_2O_3 - K_2O) + Na_2O + Ca}$ (Nesbitt & Young, 1982)

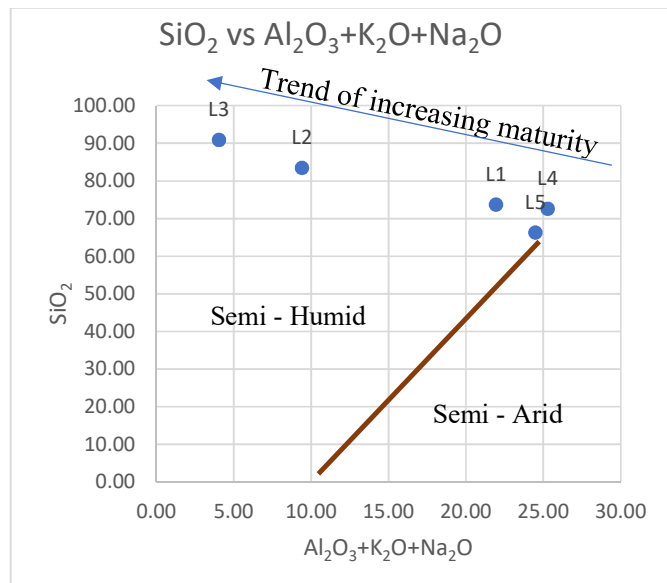
For Example, the PIA of Rock sample L1

$$PIA = \frac{(139.94 - 34.09) * 100}{(139.94 - 34.09) + 72.09 + 2.22}$$

$$= 51.59 \%$$

Plotting a graph of SiO_2 vs $(Al_2O_3 + K_2O + Na_2O)$ the maturity of the rocks samples can be graphically represented.

Graph 3.1: Representation of maturity of rocks. (Suttner & Dutta, 1986)



The given graph depicts the rock samples from L2 and L3 have the highest maturity as compared to L1, L4 and L5.

3.4 TIC and DOC data

The data obtained from the NGRI included the TIC, DIC, TOC and DOC concentrations.

Using this the PIC and POC was calculated.

Table 3.2: The constituents of the Total Carbon

Name	TC mg/l	TIC mg/l	TOC mg/l	PIC mg/l	POC mg/l	DIC mg/l	DOC mg/l
L-1	19.105	9.824	9.281	0.162	4.255	9.662	5.026
L-2	23.057	13.625	9.432	0.913	3.278	12.712	6.154
L-3	26.963	15.948	11.014	7.094	6.158	8.854	4.856
L-4	16.879	6.684	10.195	1.264	6.807	5.42	3.388
L-5	10.985	5.7	5.285	0.335	1.694	5.365	3.591

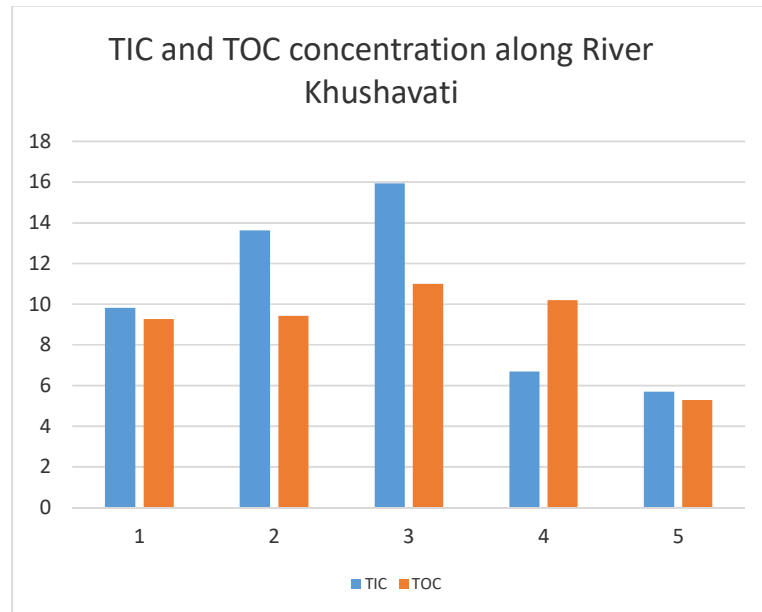
The TIC, TOC and the DIC, DOC data were provided by the TOC method conducted by NGRI.

$$\text{PIC} = \text{TIC} - \text{DIC}$$

$$\text{POC} = \text{TOC} - \text{DOC}$$

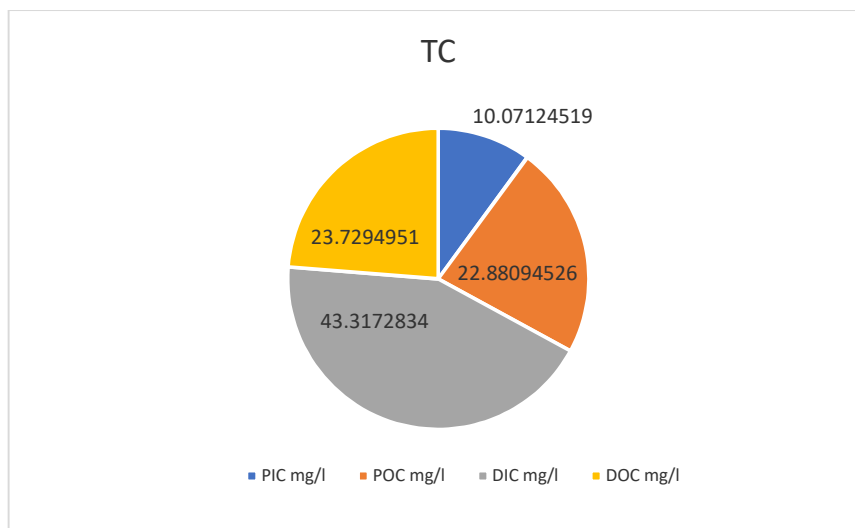
A graphical representation of the TIC and TOC was plotted so as to understand the trend along the course.

Graph 3.2: The TIC and TOC trend along the river track.



Also with this data the average percentages of the Carbon components were calculated as seen in the below pie-chart.

Graph 3.3: The percentages of the constituent Carbon



Further calculations were conducted to find the river runoff using the physical parameters of the river like width, depth, hydraulic radius and the average slope gradient of the river.

Calculation for river runoff:

The river velocity using Manning's formula = $28.57 \times Rh^{2/3} \times S^{1/2}$ (Choo, Pak, Lee, & Oh, 2011)

where Rh is the Hydraulic radius and S is the slope.

Cross sectional area of the river can be calculated using the average depth and the average width of the river. Using Google Earth imagery the average width of the River Kushavati is 32.98 metres. The average depth of the river was calculated using field data observations. The Average depth of the River Kushavati is 1.64 metres.

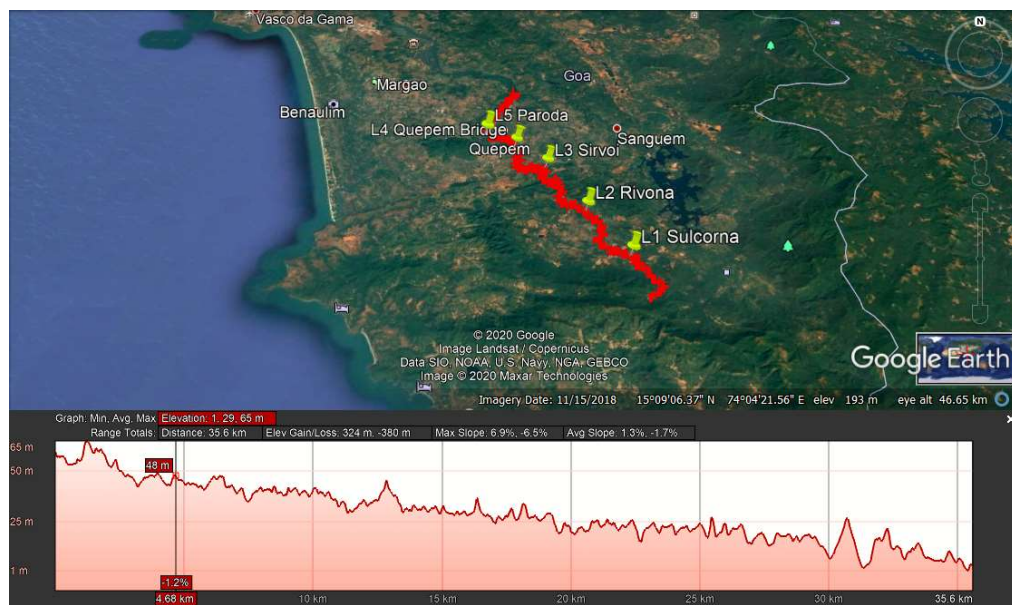


Figure 3.11: Profile along the River track in Google Earth imagery indicating the average slope

$$\text{Cross-sectional Area} = \text{Depth} \times \text{Width}$$

$$\text{The river runoff} = \text{River Velocity} \times \text{Cross-sectional Area}$$

The average seasonal runoff of the River Kushavati during the month of January i.e. the duration of the sample collection is calculated as $29.551707 \text{ m}^3 \text{ s}^{-1}$.

The Bjerrum plot (Middelburg, 2019) can be used to calculate the proportions of the DIC species. Therefore with respect to this Bjerrum plot and the average pH parameter (6); the species content of DIC was calculated.

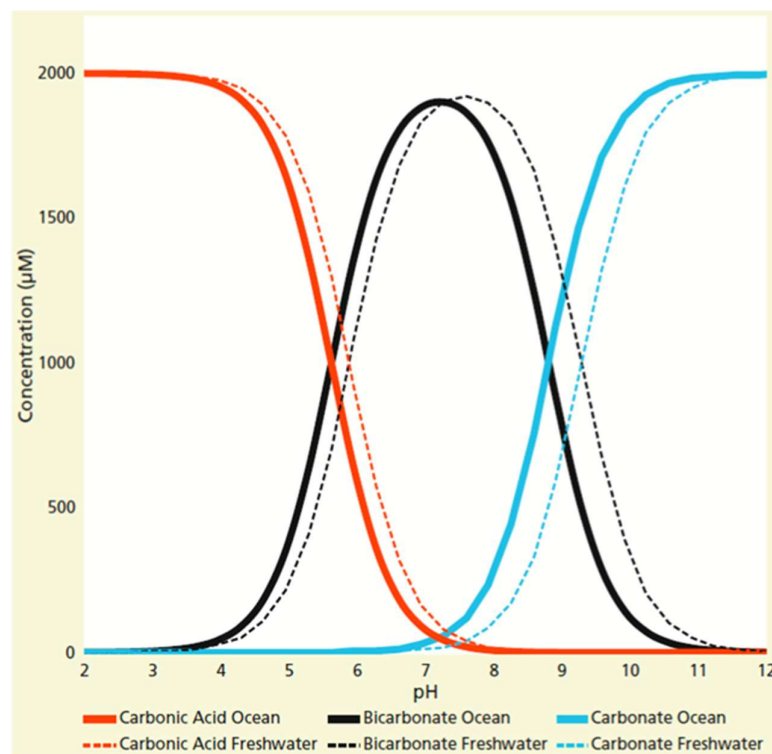


Figure 3.12: The Bjerrum Plot with the Dotted line indicating the plot for Fresh water and the Solid line being the plot for Seawater (Middelburg, 2019)

The species of DIC include CO_2 , HCO_3^- and CO_3^{2-} ; each having molecular weights of 44.01g/mol, 61.017g/mol and 60.009g/mol respectively. The proportional concentrations of the species is given by;

$$[\text{CO}_2]_{\text{eq}} = \frac{[\text{H}^+]_{\text{eq}}^2}{[\text{H}^+]_{\text{eq}}^2 + K_1 [\text{H}^+]_{\text{eq}} + K_1 K_2} \times \text{DIC},$$

$$[\text{HCO}_3^-]_{\text{eq}} = \frac{K_1 [\text{H}^+]_{\text{eq}}}{[\text{H}^+]_{\text{eq}}^2 + K_1 [\text{H}^+]_{\text{eq}} + K_1 K_2} \times \text{DIC},$$

$$[\text{CO}_3^{2-}]_{\text{eq}} = \frac{K_1 K_2}{[\text{H}^+]_{\text{eq}}^2 + K_1 [\text{H}^+]_{\text{eq}} + K_1 K_2} \times \text{DIC},$$

(Middelburg, 2019)

- Where, H^+ is calculated by the antilog of the pH (6)
- K_1 and K_2 are the H^+ values at the intersection of the $[\text{CO}_2 - \text{HCO}_3^-]$ and $[\text{HCO}_3^- - \text{CO}_3^{2-}]$ in the Bjerrum plot where $\text{pH} = -\text{Log}_{10}[\text{H}^+]$
- DIC is the average concentration of DIC in mg/L

For Example in the case of CO_2 concentration

$$\text{CO}_2 = \frac{10^{-12}}{10^{-12} + (7.94 * 10^{-13}) + (7.94 * 3.98 * 10^{-17})} * 8.4026$$

$$= 4.7 \text{ mg/L}$$

The major species of the DIC was CO_2 constituting an average of 55.72% of the total DIC thus amounting to 4.7 mg/L concentrations. HCO_3^- and CO_3^{2-} concentrations were 3.72mg/L and 0.00148mg/L respectively.

The annual DIC yield can be calculated using this data.

$$\text{Yield} = \frac{\text{River Runoff} * \text{Concentration} * \text{Total seconds in a year}}{\text{Molecular Weight} * \text{Area of Watershed}} \quad (\text{Takuya, et al., 2015})$$

$$\text{For CO}_2 \text{ the yield} = \frac{29.551707 * 4.7 * 31104000}{44.01 * 661}$$

$$= 147938.534 \text{ mols Km}^{-2} \text{ y}^{-1}$$

Similarly the yield for HCO_3^- and CO_3^{2-} are 84758.22014 and 34.30880756 respectively. The DIC yield across the river is sum of the yield of the three species i.e.

$$= 2.33 \times 10^5 \text{ mols km}^{-2} \text{ y}^{-1}$$

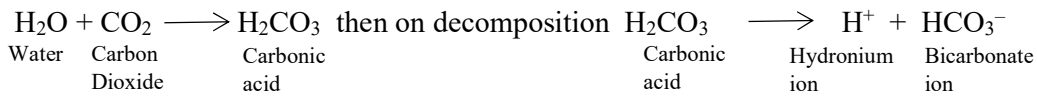
Chapter 4

Discussion

4.1 Weathering of Feldspars

Feldspar is the principal component of the Earth's crust. They are present in the three major rock divisions; Igneous, Sedimentary and Metamorphic rocks; thereby making the most abundant mineral on the planet. They make up around 60% of the earth's crust, including soils and clays. Feldspars are distinguished by the presence of Aluminium and Silica in their chemistry. The common minerals present in this group are Orthoclase, Microcline, Plagioclase and Albite. They are the principal components in rock classification schemes.

Rocks are frequently subjected to weathering which takes place on or close to the surface of the Earth. There are two main types of weathering; Physical and chemical weathering. While physical weathering may mostly involve sudden changes in temperature it can also be due to sudden change in pressure and the growth of salt crystals in cracks as the water evaporates. Chemical weathering is a result of the chemical changes that a mineral undergoes if the mineral is unstable on exposure to surface condition. These changes are highly specific to the minerals, surface conditions and the environment they are exposed to. Some minerals like quartz are almost unaffected by chemical weathering. The important surficial characteristic that leads to chemical weathering is the presence of water (both on the surface and in the atmosphere), abundance of oxygen in the atmosphere and the presence of carbon dioxide in the atmosphere. The following components when combined gives weak carbonic acids. This process which is fundamental in the chemical weathering of rocks can be given by;



This equation as we will see later in this chapter will be the base for all other equations corresponding to the chemical weathering of feldspar via dissolution.

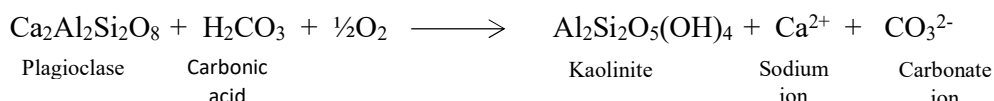
The weathering of feldspar is a major step in the geological cycling of the upper continental crustal material. It also has a greater influence on many near surface processes, including the carbon cycle. The weathering of feldspars usually occur through chemical weathering. Feldspar weathering occurs via dissolution of all components into solution, with the subsequent precipitation of the secondary minerals, this process is called hydrolysis. The overall rate of feldspar weathering is controlled by the rate of feldspar dissolution.

Dissolution of the feldspar into solution should usually result in the stoichiometric release (in the same proportion as that of the elements in the mineral) of the components of feldspar. However, dissolution is usually non stoichiometric during the initial phase. This is due to the exchange and adsorption/de-adsorption reactions that occur as soon as the fresh feldspars surface is placed in solution.

Feldspars of all compositions have an experimental dissolution rate which increases with increasing H^+ activity at $\text{pH} < 6$, and increasing OH^- activity at $\text{pH} > 8.5$, a pattern typical of many silicate minerals. The average pH of the river water in the River Khushavati is 6 thus being acidic. In the acidic pH region ($<\text{pH } 6$) albite and K-feldspar have nearly identical experimental dissolution rates, with the dissolution rate (R) proportional to $[\text{H}^+]^{0.5}$. This is in

contrast to the observation in natural soils that albite weathers much more rapidly than K-feldspar.

The overall feldspar weathering process can be simplified as the alteration of feldspar to common clay minerals, such as kaolinite. The reaction can be given as;



In the above reaction we can see Calcic Plagioclase undergoing a reaction and getting altered to Kaolinite. But similar reaction can be made for other feldspar minerals. The ions of Calcium and carbonate that are obtained through this reaction can also react under suitable conditions to form Calcium carbonate or Calcite. Also, the carbonate ions can give rise to carbon dioxide. Thereby, affecting the carbon cycle over a vast time span (>1 My).

The rate of Feldspars dissolution reaction is neither dependant on the characteristic of the bulk solution, nor do the chemistry and structure control the rate of the reaction. Infact, it is dependent on how the mineral surface and solution react at the mineral-water interface.

Feldspar weathering via dissolution is among the most thoroughly studied of the known minerals. This is partly due to the abundance of feldspars in the Earth's crust. Over the years, there has been more vigorous study of this topic. Some of the reasons for this increased interest in feldspar weathering are:

- To improve our understanding of the effects of acid precipitation, and the long-term capacity of soils to neutralize anthropogenic acidic rainfall (e.g. Reuss and Johnson, 1986).
- To study the importance of silicate weathering in regulating atmospheric CO₂ concentration over geologic time, and thereby control global climate change(e.g. Walker et al., 1981; Berner, et al. 1983; Lasaga et al., 1985; Yolk, 1987).
- To create reactive transport models using chemical kinetics, which require rate laws for the dissolution and precipitation of major minerals.
- The tremendous advances in surface science and heterogeneous kinetics which have provided both new analytical and theoretical techniques, allowing progress on complex problems of heterogeneous kinetics such as feldspar dissolution.

The plagioclase identification under the micro-sections in majority of the sample sites i.e. in L1, L4 and L5 and the presence of Ca in the XRF data indicates the contribution of formation of carbonates in the deep oceans on reaction with the CO₃²⁻ species of the DIC. Thus inferring the effect these Granito-Gneissic rocks can have on the carbon consumption.

The weathering indices like CIA and PIA indicate the degree of weathering (Nesbitt & Young, Early Proterozoic Climate and Plate motion inferred from major element chemistry of lutites, 1982). The two rock samples of location L2 and L3 have high CIA and PIA values and are siliciclastic sedimentary rocks belonging to the Semi-Humid environment as inferred from the SiO₂ vs Al₂O₃ + K₂O + Na₂O (Suttner & Dutta, 1986). This environment indicates the rock samples of L1 and L2 have contributed to the chemical weathering in the past and

have attained a very high chemical maturity i.e. these samples will have insignificant role in the further weathering. The majority of the rock samples have low CIA and PIA values and are of Granito-Gneissic type. The low CIA and PIA values of the rock specimen of locations L1, L4 and L5 range from 51.19 to 54.73 and 51.59 to 58.03 respectively; indicating that these samples that are least mature have a higher degree of scope for further weathering thus contributing to the process of carbon consumption.

4.1.2 Residence time and the DIC yield

In the River Kushavati the DIC content is 43.32% thus comprising a majority of the total carbon content. As quoted in the book titled '*The Global Water Cycle*' by Berner, the residence time of DIC in river water is highest among the other constituents of the total carbon amounting to 83000 years. The high ratio of DIC content concludes the river as a carbon sink.

The net DIC yield of the River Kushavati is 2.33×10^5 mol km $^{-2}$ y $^{-1}$. This is comparable to the DIC yield of the Nethravati watershed which is 3×10^5 mol km $^{-2}$ y $^{-1}$ (Gurumurthy, Balakrishna, & Udaya, 2013) and the watershed systems of the Voltri Massifs in Italy ($3.02 \pm 1.67 \times 10^5$ mol km $^{-2}$ y $^{-1}$) (Frondini, Vaselli, & Zuccolini, 2019). The Yield is much lower than rivers draining from mountainous ranges like Bhagirathi-Alaknanda (4×10^5 mol km $^{-2}$ y $^{-1}$) (S, Singh, & TK, 1999), Yamuna (5×10^5 mol km $^{-2}$ y $^{-1}$) (Dalai TK, 2002) and also to the high annual DIC yield of the Western Ghat region which is the 9th largest DIC contributor in the world and amounts to 15.47×10^5 mols km $^{-2}$ y $^{-1}$ (Reddy, Gupta, & Reddy, 2019). This indicates that the gradient and the terrain play a major role in the carbon consumption rate. The DIC yield in the Kushavati is much higher than the River Parana (0.9

$\times 10^5$ mol km $^{-2}$ y $^{-1}$), Amazon (0.5×10^5 mol km $^{-2}$ y $^{-1}$), Congo-Zaire (0.5×10^5 mol km $^{-2}$ y $^{-1}$) and Orinoco (0.6×10^5 mol km $^{-2}$ y $^{-1}$), (Gaillardet, Dupre, & Allegre, 1999). This DIC yield estimates the DIC contribution of the rivers to the sea. The study area being along the track of a major tributary, the DIC yield of River Kushavati will contribute to the DIC content of the River Zuari.

Chapter 5

Conclusion

The quantity of CO₂ as a greenhouse gas has impacted the global temperatures tremendously. Over geologic timescales there were series of extreme heating and cooling of the Earth at different times. The atmospheric carbon content played an important role in the global temperatures at that time. The geochemical weathering of rocks is a major carbon sink having a crucial role on the atmospheric carbon content. Studies have been conducted on major rivers with the underlying geology being carbonates and of mafic origin but those of Granito-Gneissic type is least studied.

To understand the weathering of Granito-Gneissic rock and its role on the global carbon cycle on a long timescale, the hydrogeochemistry of the rock samples and the river water of the River Kushavati is studied. The effects of these rock types on the carbon consumption rate is a need. The majority of the rock samples collected along the track of the River Kushavati composed of high plagioclase content indicating the major role the granitic rocks can have on the geochemical weathering and the contribution of Ca cations. Also the surrounding rocks have a very high scope for further weathering as the majority of the collected rock samples were fairly immature.

The high average DIC content confirms the river as a negative feedback to the atmospheric carbon and indicates the contribution of DIC supply in the Arabian Sea via River Zuari. The aqueous CO₂ comprises of 55.72% of the DIC. This high CO₂ content contributes to the low pH of the river water which in turn leads to the increase in the silicate weathering rate. The DIC yield is nearly half the DIC yield of mountainous rivers like Yamuna and Bhagirathi-

Alaknanda but nearly 4 times that of major world rivers like the Amazon, Orinoco and Parana which is very high considering the river to be a tributary.

Besides photosynthesis weathering is a major absorber of atmospheric carbon. Thus greater emphasis should be laid on studies related to hydrogeochemistry. Goa being geologically one of the least explored, this research contributes to the study of the rock types of the area. The Hydro geochemical study will contribute to the understanding of weathering effects the southwestern rivers of India will have on the Pre Cambrian silicate rocks of the Dharwar craton.

Bibliography

- Berner, E. K., & A., B. R. (1987). *The Global Water Cycle*. Prentice Hall.
- Berner, R. A. (1992, August). Weathering, plants, and the long-term carbon cycle. *Geochimica et Cosmochimica Acta*, 56(8), 3225-3231. doi:10.1016/0016-7037(92)90300-8
- Berner, R. A. (2004). The Phanerozoic Carbon Cycle.
- Berner, R. A., & Caldeira, K. (1997). The need for mass balance and feedback in the geochemical carbon cycle. *Geology*, 955-956. doi:10.1130/0091-7613(1997)025<0955:TNFMBA>2.3.CO;2
- Berner, R. A., & Lasaga, A. C. (1989, March). Modelling the Geochemical Carbon Cycle. *SCIENTIFIC AMERICAN*, 260(3).
- Brady, P. V. (1991). The Effect of Silicate Weathering on Global Temperatures and CO₂. *Journal of Geophysical Research*, Chapter 5.
- Bruckner, M. Z. (2016, November 23). *Measuring Dissolved and Particulate Organic Carbon (DOC and POC)*. Retrieved from serc.carleton.edu: https://serc.carleton.edu/microbelife/research_methods/biogeochemical/organic_carbon.html
- CAO, J., YUAN, D., GROVES, C., HUANG, F., YANG, H., & LU, Q. (2012, August 08). Carbon Fluxes and Sinks: the Consumption of Atmospheric and Soil CO₂ by Carbonate Rock Dissolution. *ACTA GEOLOGICA SINICA*, 86(04), 963-972. doi:10.1111/j.1755-6724.2012.00720.x
- Choo, H. T., Pak, S. K., Lee, S. J., & Oh, R. S. (2011). Estimation of river discharge using mean velocity equation. *KSCE Journal of Civil Engineering*, 927-938.

Dalai TK, K. S. (2002). Major ion chemistry in the headwaters of the Yamuna river system: chemical weathering, its temperature dependence and CO₂ consumption rates. *Geochimica et Cosmochimica Acta*, 66, 3397–3416.

Desai, A. (2011). The Geology of Goa Group: Revisited. *JOURNAL GEOLOGICAL SOCIETY OF INDIA*, 233-242.

Frondini, F., Vaselli, O., & Zuccolini, M. V. (2019). Consumption of Atmospheric Carbon Dioxide through Weathering of Ultramafic Rocks in the Voltri Massif (Italy): Quantification of the Process and Global Implications. *Geosciences*, 1-22. doi:10.3390/geosciences9060258

Gaillardet, J., Dupre, B., & Allegre, C. (1999). Global silicate weathering and CO₂ consumption rates deduced from the chemistry of large rivers. *Chemical Geology*, 159, 3-30.

Gierke, J. S. (2002). River Velocity. In *ENG5300 Engineering Applications in the Earth Sciences*. Houghton.

Gurumurthy, G. P., Balakrishna, K., & Udaya, S. H. (2013). Major ion, trace element and organic carbon geochemistry of river Nethravati, Southwest coast of India. In G. P. Gurumurthy, K. Balakrishna, & S. H. Udaya, *Chapter 3: SILICATE WEATHERING, CO₂ CONSUMPTION AND ITS RATE CONTROL PARAMETERS IN A HUMID TROPICAL RIVER BASIN, SOUTHWESTERN INDIA* (pp. 35-56). Manipal University: Shodhganga.

Kawahata, H., Kazuhiko, F., Akira, I., Mayuri, I., Shinya, I., Azumi, K., . . . Atsushi, S. (2019). Perspective on the response of marine calcifiers to global warming and ocean acidification—Behavior of corals and foraminifera in a high CO₂ world “hot house”. *Progress in Earth and Planetary Science*.

Middelburg, J. J. (2019). *Biogeochemical Processes and Inorganic Carbon Dynamics*.

Utrecht: ResearchGate.net. doi:DOI: 10.1007/978-3-030-10822-9_5

Moody, C., Worrall, F., Howden, N. K., & Burt, T. P. (2012). *The loss of DOC in transit through river catchments - impact on the atmosphere and understanding trends*. American Geophysical Union.

Nesbitt, H. W., & Fedo, C. M. (n.d.). *Quartz and Feldspar stability, steady and non-steady state weathering, and petrogenesis of siliciclastic sands and muds*.

Nesbitt, H., & Young, G. (1982). Early Proterozoic Climate and Plate motion inferred from major element chemistry of lutites. *Nature* 299, 715 – 717.

Nesbitt, H., Young, G., McLennan, S., & Keays, R. (1996). Effects of chemical weathering and sorting on the Petrogenesis of Siliciclastic Sediments with Implications for provenance studies. *Journal of Geology*, 525 – 542.

Raoul, G. N., Brunet, F., Probst, J., & Boeglin, J. I. (2007). *Soil and atmospheric controls on the $\delta^{13}\text{C}$ of riverine dissolved inorganic carbon in the Nyong river basin (South Cameroon)*.

Reddy, S. K., Gupta, H., & Reddy, V. (2019). Dissolved inorganic carbon export by mountainous tropical rivers of the Western Ghats, India. *Chemical Geology*, 530. doi:10.1016/j.chemgeo.2019.119316

S, K., Singh, S. K., & TK, D. (1999). Silicate weathering in the Himalaya: Role in contributing to major ions and radiogenic Sr to the Bay of Bengal. . *In Ocean Science, Trends and Future Directions* (pp. 23-51). New Delhi: Indian National Science Academy and Academia International.

- SHETYE, S. R., GOUVEIA, D. A., SINGBAL, Y. S., NAIK, G. C., SUNDAR, D., MICHAEL, S. G., & NAMPOOTHIRI, G. (1995). Propagation of tides in the Mandovi-Zuari estuarine network. In *Earth Planet. Sci.* (pp. 667- 682). Indian Academy of Science.
- Suttner, L. J., & Dutta, P. K. (1986). Alluvial sandstone compositin and paleoclimate, I. Framework mineralogy. *Journal of Sedimentary Petrology*, 329 - 345.
- Takuya, M., Souya, O., Akihiko, I., Atsushi, S., Thura, A., Raywadee, R., . . . Hodaka, K. (2015). Chemical weathering and long-term CO₂ consumption in the Ayeyarwady and Mekong river basins in the Himalayas . *Journal of Geophysical Research: Biogeosciences*, 1165 -1175.
- White, A. F., Susan, L., & Brantley. (1995). *Chemical Weathering Rates of Silicate Minerals*.
- Wilson, M. J. (2004). *Weathering of the primary rock-forming* .
- Zhang, L., Qin, X., Huang, Q., & Liu, P. (2019). Role of sulfuric acid in chemical weathering of carbonate rocks for evaluating of carbon sinks in the Yangtze River Basin, China. *E3S Web of Conferences*, 1-5. doi:10.1051/e3sconf/20199806015